

## Interfacial analysis of chitosan/bone: cortical and cancellous bone matrices

C.V. Paz López, S.R. Vasquez-Garcia

*Department of Chemistry, Universidad Michoacana de San Nicolás de Hidalgo  
Morelia, Mich. 58060, México*

N. Flores-Ramirez \*

*Department of Wood Engineering and Technology, Universidad Michoacana de San Nicolás de Hidalgo  
Morelia, Mich. 58060, México*

(Received: June 28th, 2015; Accepted: July 20th, 2016)

Thermal stability and phase separation of a film on a substrate can be controlled at the interface level by changing the compatibility between both components, which is based on molecular interactions. Thus, in this study chitosan was used as a coating agent due to its superior film-forming properties and multiple molecular interactions with bone. In particular, two types of bone substrates were considered to study the bio-adhesion phenomena: cancellous and cortical bones. Firstly, chitosan/bone samples were prepared by controllable dip-coating method under fixed conditions, and subsequently an experimental investigation was utilized to analyze the interfacial compatibility and interaction between chitosan with the two bone substrates. As a result, Fourier transform infrared spectroscopy (FTIR) data revealed a strong interaction between the chitosan molecules and bones. Meanwhile, by scanning electron microscope (SEM) and microhardness analysis a moderate interfacial compatibility was exhibited. Furthermore, analyses by X-ray diffraction were used to identify the spatial arrangement of chitosan structure on bone, which was increased as a result of an increase in acidity of chitosan solution.

### Introduction

Disorders such as arthritis, osteoporosis, osteonecrosis, bone tumor and bone fracture due to illness and trauma affect hundreds of millions of people across the world [1]. Particularly, osteoporosis is characterized by low bone mass that often results in fracture, the majority of these fractures occur in elderly patients [2].

In recent years, there have been researched on using biomaterials to treat bone loss or failure, because when they are used in human and animals, these are able to repair and positively influence the growth of cells [3]. Chitosan (Cs) is a very useful biomaterial in orthopedics for its excellent biocompatibility and physical properties, allowing to be applied in bone tissue engineering. Thus, this polymer has been widely used in bone regeneration alone or in combination with various materials. Beside Cs also has demonstrated antiseptic and antibacterial activities and its integration to bone do not represent septic problems [4].

Cs has potential for use in regenerative medicine to restore the functions of damaged tissues and organs. This has fostered the study of this biopolymer in artificial tissues, including bone, cartilage, nerves, blood vessels and skin. The knowledge of chemistry and biochemistry of Cs has given as result the use of this biopolymer in repairing or replace of diseased or wounded tissues [5].

The benefits that Cs offers to bone are attributed to its chemical structure. Cs is a copolymer of  $\beta$ [1 $\rightarrow$ 4]-linked 2-acetamido-2-deoxy-D-glucopyranose and 2-amino-2-deoxy- $\beta$ -D-glucopyranose generally obtained by alkaline deacetylation of chitin [6]. These properties contrast with bone characteristics.

Bone is a complex biological material that contains between 10 and 20 wt% water. From the dry mass,

approximately from 60 to 70 wt% is bone mineral and the rest is mainly a collagen fiber protein [7, 8]. The crystal mineral phase is constituted of hydroxyapatite (HA), which is characterized by the presence of  $\text{OH}^{-1}$  and  $\text{PO}_4^{-3}$  ions [9].

All bones contain a compact and dense outer shell of cortical bone (CorBn), and a spongy structure named cancellous bone (CanBn), whose structures are composed of lamellas containing only subtle differences. The CorBn lamella presents repeating sets of unidirectional orientations, while the CanBn lamella shows one of the two unidirectional fibril sets, some of which are aligned with the long axis of the individual trabecular strut. Additionally, CanBn contains less mineral than CorBn [10, 11].

In relation to the above mentioned Cs and bone show surfaces of different nature, for this reason they represent a suitable opportunity to analyze the interface behavior between. Therefore, the aim of this work is to study the interaction between Cs (thickness less than 0.1  $\mu\text{m}$ ) and a cow bone, in a system that mimics the human bone.

### Materials and methods

#### *Preparation of Cs thin films*

Filmogenic Cs solutions were prepared by mixing acetic acid (AC) with Cs for 1 h at room temperature. These solutions were labeled according to the amount of Cs used (wt%), follows by the molarity of each AC solution (Table 1). Each one of these solutions were poured into plastic petri dishes (10 mL), and placed in an oven and dried for 30 h at 50 °C (0.60 atm) until a constant weight was obtained.

#### *CS films on cancellous and cortical bones*

CanBn and CorBn specimens were obtained from the hip

\* [fr\\_nelly@yahoo.com](mailto:fr_nelly@yahoo.com)

**Table 1.** Cs filmogenic solutions for films preparation

Label	Cs (wt%)	Acetic acid solution		Cs/AC solution pH
		Molarity	pH	
1.17 Cs	1	0.17	3.05	4.59
1.30 Cs	1	0.30	2.89	4.63
3.17 Cs	3	0.17	3.05	4.9
3.30 Cs	3	0.30	2.89	4.69
7.17 Cs	7	0.17	3.05	6.51
7.30 Cs	7	0.30	2.89	5.58

of a healthy cow (3 years of age, 275 kg). These specimens were subjected to a mechanical treatment to remove the organic tissue. Then, the bare bones were cut into small pieces ( $1.0 \times 0.5 \times 0.30 \text{ cm}^3$ ), which were coated using programmed equipment, with dip-coating speed of 20 mm/s with a residence time of 5 sec and 4 cycles of repetition. After that, the coating pieces were dried in a vacuum oven at 50 °C (0.60 atm) for 30 h.

### Characterization

Fourier transform infrared (FTIR) spectra were obtained under standard ambient conditions (25 °C, 0.987 atm) in a Bruker Tensor 27 FTIR, with a wave number range of 400 - 4000  $\text{cm}^{-1}$  by ATR. The deacetylation percent of Cs was calculated using the equation Brugnott [12].

The surface morphology was analyzed by scanning electron microscopy (SEM) in a JEOL JSM-5300 electron microscope under a resolution of 100 nm. Previous to the SEM analysis, the samples were coated with graphite.

Microhardness measurements were carried out by means of a LEITZ WETZLAR tester (7756 model). The pre-treatment consisted in dipping the sample into commercial resin, after curing a mirror-polishing process was applied. The tests were carried out under standard ambient conditions. The microindentation was held for 5sec with an applied load (P) at 0.025 Kgf. On each sample, 7 microindentation tests were performed.

Diffraction patterns of the samples were observed by diffraction X-ray (DRX) using an X-ray diffractometer Bruker D8 Advance with primary Göbel mirror optics and scintillation detector. The wavelength was 1.5406 Å of Cu  $K_{\alpha 1}$  with 40 kV and 40 mA. Database Powder Diffraction File (PDF-2) International Center of Diffraction Data (ICDD) was used to identify the present phases.

## Results and discussion

### Structural analysis by FTIR

Figure 1 shows the FTIR spectra of all Cs dry films. Inset A and B show the zoomed view around 3120 and 1600  $\text{cm}^{-1}$  respectively, which correspond to absorptions of OH and NH groups. In both cases, the highest and lowest intensity corresponded to the 1.17Cs and 3.17Cs films, respectively.

The film 1.17Cs exhibited the largest number of free polar groups and the film 3.17Cs presented the lowest number of these groups (with highest intramolecular interactions).

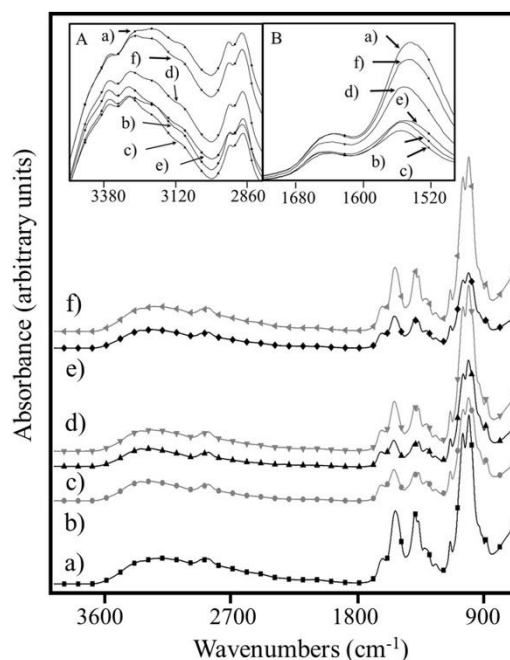


**Figure 1.** FTIR spectra of a) 1.17Cs, b) 1.30Cs, c) 3.17Cs, d) 3.30Cs, e) 7.17Cs and f) 7.30Cs. Inset A and B are a zoomed view in the range of 3120 and 1600  $\text{cm}^{-1}$  respectively.

In order to relate the mechanical behavior with the Cs/bone interaction response the 3.17Cs and 3.30Cs films were selected. Based on FTIR data, the degree of deacetylation of Cs was confirmed about 81.77 %.

According to Figure 2, signals were related to the hydroxyapatite phase. The band at 1022  $\text{cm}^{-1}$  was assigned to  $\text{PO}_4^{3-}$ , where the highest intensity was shown for CorBn; so due to collagen, signals at 1550 and 1240  $\text{cm}^{-1}$  showed the presence of organic phase derived of existence of primary and tertiary amides respectively [13, 14].

Figures 3 and 4 show the FTIR results of Cs/CanBn and Cs/CorBn respectively. In both cases, the 1022  $\text{cm}^{-1}$  signal (assigned to  $\text{PO}_4^{3-}$ ) decreased by the Cs addition, where samples such as 3.30Cs/CanBn and 3.17Cs/CorBn exhibited the lowest intensities.

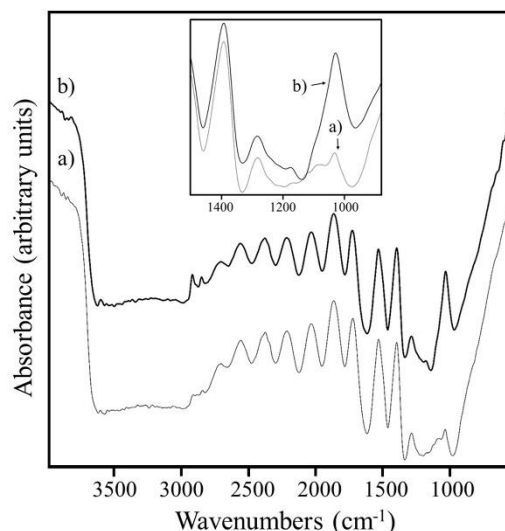


**Figure 2.** FTIR spectra of a) CanBn and b) CorBn.

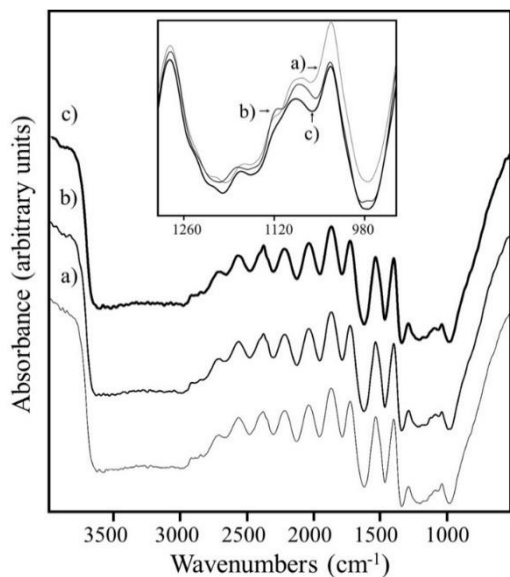


Figure 3. FTIR spectra of a) CanBn, b) 3.17Cs/CanBn and c) 3.30Cs/CanBn.

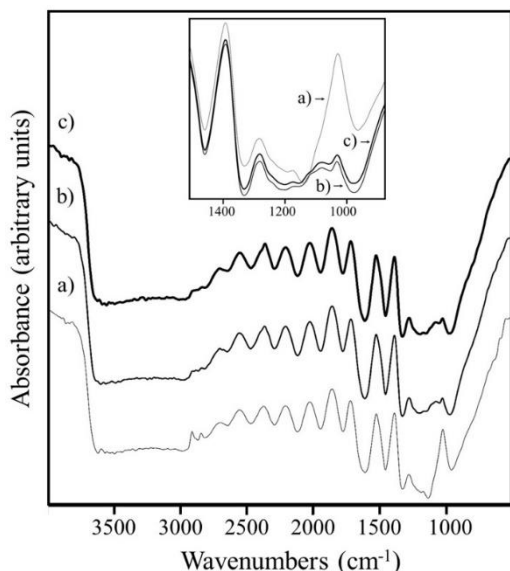


Figure 4. FTIR spectra of a) CorBn, b) 3.17Cs/CorBn and c) 3.30Cs/CorBn.

*Morphological analysis of Cs films, by SEM*

Figure 5 shows the SEM analysis of Cs films, where some agglomerations were due to high Cs concentration.

The thickness as function of Cs and AC concentration are presented in Figure 6 and Table 2. The highest and lowest values of Cs were obtained at 7 and 1 wt% of Cs respectively. As consequence of the high AC concentration (0.30 M) the values of thickness decreased. This was because the Cs molecules were arranged closely due to an excess of AC.

*Mechanical analysis by microhardness*

Microindentation hardness testing was performed on Cs/CanBn and Cs/CorBn samples (Table 3). For the CanBn, the sample 3.17Cs/CanBn showed the highest hardness. It was 25.76 % harder than the uncoated bone. After this value, the hardness decreased as effect of an increment in Cs concentration.

Table 2. Cs films thicknesses determined by SEM.

Cs film	Average thicknesses (µm)	Thickness change (%)*
1.17Cs	7.20	---
3.17Cs	16.0	222.22
7.17Cs	28.0	388.00
1.30Cs	18.0	--
3.30Cs	20.0	111.11
7.30Cs	24.0	133.33

\* Regarding the first filmogenic solution.

The sample 3.30Cs/CorBn showed the highest hardness, which was 16.58 % harder than the uncoated bone, from 35.65 to 41.56 GPa. This increase in hardness indicates the associations of Cs molecules, as well as the association of Cs molecules with bone. Thus, penetration resistance was the result of a tight arrangement between Cs chains.

*Phase analysis, XRD of bone and covered bone*

XRD patterns of Cs/bone samples are shown in Figure 7. The existence of Cs in the sample was clearly revealed for signal at 20°. This crystalline signal was more notorious for the 3.17Cs/CanBn and 7.30Cs/CanBn samples. However, for the sample 1.30Cs/CanBn did not exist a detectable signal, indicating the absence of crystalline phases. The other signals were characteristics of the compact hexagonal crystal structure of hidroxiapatite [15, 16]. Additionally, strong signals of crystallinity are presented in 1.17Cs/CanBn, 3.17Cs/CanBn, 3.30Cs/CanBn, 7.17Cs/CanBn and 7.30Cs/CanBn samples. Thus, the crystallinity was increased as consequence of an increase in the AC concentration.

Figure 8 shows the XRD patterns of CorBn 3.17Cs/CorBn

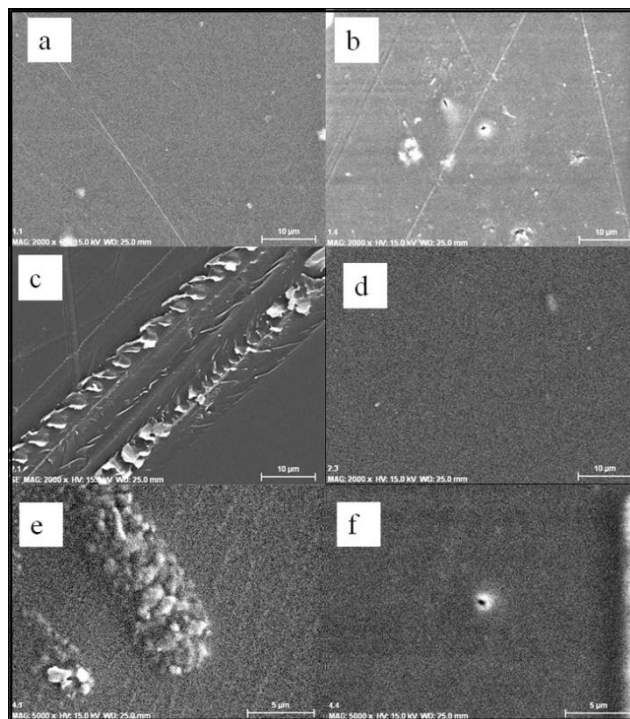
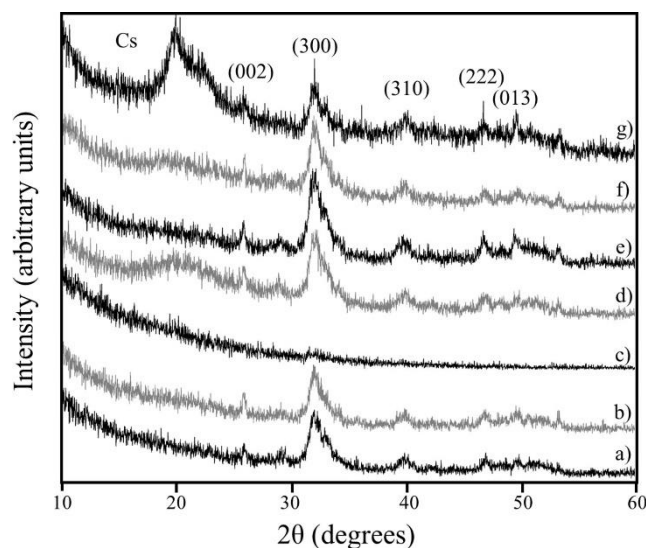


Figure 5. SEM micrographs a) 1.17Cs, b) 1.30Cs, c) 3.17Cs and d) 3.30Cs (at 2000×), e) 7.17Cs and f) 7.30Cs (at 5000×).

**Table 3.** Microhardness of coated and uncoated bones

Coating Bone	Microhardness(GPa)		Percent difference of micro-hardness (%)
	Bone Uncoated	Bone Coated	
1.17Cs/CanBn	28.34	29.84	5.29
1.30Cs/CanBn	28.34	34.44	21.521
3.17Cs/CanBn	28.34	35.64	25.76
3.30Cs/CanBn	28.34	22.05	-22.19
7.17Cs/CanBn	28.34	18.3	-35.43
7.30Cs/CanBn	28.34	19.5166	-31.13
3.17Cs/CorBn	35.65	34.67	-2.75
3.30Cs/CorBn	35.65	41.56	16.58



**Figure 7.** XRD patterns of a) CanBn, b) 1.17Cs/CanBn, c) 1.30Cs/CanBn, d) 3.17Cs/CanBn, e) 3.30Cs/CanBn, f) 7.17Cs/CanBn and g) 7.30Cs/CanBn.

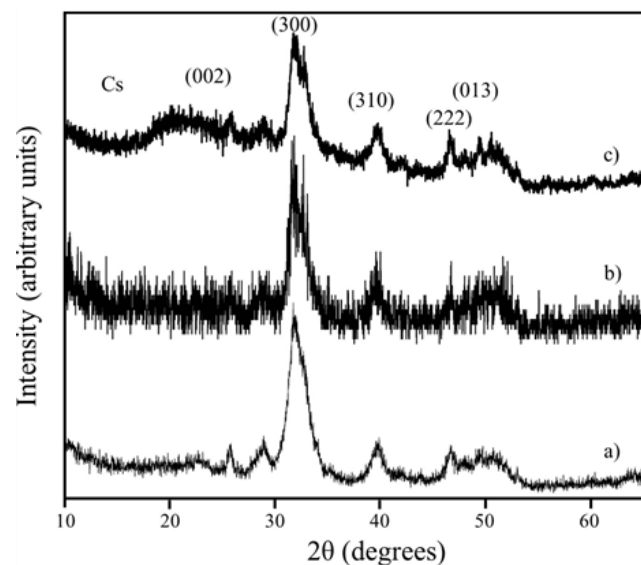


**Figure 8.** XRD patterns of a) CorBn, b) 3.17Cs/CorBn and c) 3.30Cs/CorBn.

and 3.30Cs/CorBn. These results gave evidence of the presence of Cs, indicating that Cs has been embedded into the bone matrix. Moreover, it was observed that crystallinity was increased because of AC concentration. Thus, the 3.30Cs/CorBn exhibited the higher crystallinity.

**Conclusions**

The presence of inter- and intramolecular forces of attraction improved the orientation of chitosan chains. It occurred at intermediate chitosan concentrations (i.e. 3.17Cs and 3.30Cs), where the number of free polar groups were lower than other samples. According to this, for CanBn and CorBn the highest crystallinity on both surfaces was observed at intermediate chitosan concentrations (i.e. 3.17Cs/CanBn and 3.30Cs/CorBn). These results were also consistent with the increase of the hardness values, since in our study the 3.17Cs/CanBn and 3.30Cs/CorBn samples increased their hardness 25.76 % and 16.58 % respectively, in relation to the uncoated bone.

**Acknowledgment**

Financial support from the National Council of Science and Technology (CONACyT-Mexico) under the grant approved #61414 and 104257, PROMEP Collaborative Thematic Networks. Coordination of Scientific Research (UMSNH) and CIC-UMSNH are gratefully acknowledged.

**References**

- [1]. S. Bose, S. Tarafder, *Acta Biomater.* **8**, 1401 (2012).
- [2]. N.H Kelly, J.C. Schimenti, F.P. Ross, M.C.H. Van der Meulen, *Bone* **68**, 1 (2014).
- [3]. S. Tang, B. Tian, Y.J. Guo, Z. Zhu, Y.P. Guo, *Surf. Coat. Tech.* **251**, 210 (2014).
- [4]. M. Dash, F. Chiellini, R.M. Ottenbrite, E. Chiellini, *Prog. Polym. Sci.* **36**, 981 (2011).
- [5]. R.A.A. Muzzarelli, *Carbohydr. Polym.* **83**, 1433 (2011).
- [6]. J. Berger, M. Reist, O. Felt, R. Gurny, *Eur. J. Pharm. Biopharm.* **57**, 35 (2004).
- [7]. B. Burton, A. Gaspara, D. Josey, J. Tupy, M.D. Grynypas, T.L. Willett, *Bone* **61**, 71 (2014).
- [8]. J. Black, G. Hastings, *Handbook of biomaterial properties (Springer Science & Business Media 2013)* pp 2-98.
- [9]. A. Bigi, G. Cojazzi, S. Panzavolta, A. Ripamonti, N. Roveri, M. Romanello, K.N. Suarez, L. Moro, *J. Inorg. Biochem.* **68**, 45 (1997).
- [10]. N. Reznikov, R. Shahar, S. Weiner, *Acta Biomater.* **10**, 3815 (2014).
- [11]. J.B. Lynch, P.D. Spence, D.E. Baker, T.A. Postlethwaite, *J. Appl. Polym. Sci.* **71**, 319 (1999).
- [12]. J. Brugnerotto, J. Lizardi, F.M. Goycoolea, W Argüelles-Monal, J Desbrières, M Rinaudo, *Polymer* **42**, 3569 (2001).
- [13]. O. Gunduz, C. Gode, Z. Ahmad, H. Gökçe, M. Yetmez, C. Kalkandelen, Y.M. Sahin, F.N. Oktar, *J. Mech. Behav. Biomed. Mater.* **35**, 6 (2014).
- [14]. A. Pieleesz, *Spectrochim. Acta Mol. Biomol. Spectrosc.* **118**, 287 (2014).
- [15]. E. Kusriani, M. Sontang, *Radiat. Phys. Chem.* **81**, 118 (2012).
- [16]. J. Safari, L. Javadian, *Ultrason. Sonochem.* **22**, 341 (2015).